

X-ray powder diffraction study of synthetic Palmierite, $K_2Pb(SO_4)_2$

Ralph G. Tissot and Mark A. Rodriguez

Sandia National Laboratories, Materials Characterization Department 1822, Albuquerque, New Mexico, 87185

Diana L. Sipola and James A. Voigt

Sandia National Laboratories, Ceramic Materials Department 1843, Albuquerque, New Mexico, 87185

ABSTRACT

Palmierite ($K_2Pb(SO_4)_2$) has been prepared via a chemical synthesis method. Intensity differences were observed when X-ray powder data from the newly synthesized compound were compared to the published powder diffraction card (PDF) 29-1015 for Palmierite. Investigation of these differences indicated the possibility of preferred orientation and/or chemical inhomogeneity affecting intensities, particularly those of the basal (00ℓ) reflections. Annealing of the Palmierite was found to reduce the effects of preferred orientation. Electron microprobe analysis confirmed K:Pb:S as 2:1:2 for the annealed Palmierite powder. Subsequent least-squares refinement and Rietveld analysis of the annealed powder showed peak intensities very close to that of a calculated Palmierite pattern (based on single crystal data), yet substantially higher than many of the PDF 29-1015 published intensities. Further investigation of peak intensity variation via calculated patterns suggested that the intensity discrepancies between the annealed sample and those found in PDF 29-1015 were potentially due to chemical variation in the $K_2Pb(SO_4)_2$ composition. X-ray powder diffraction and crystal data for Palmierite are reported for the annealed sample. Palmierite is Trigonal/Hexagonal with unit cell parameters $a = 5.497(1)$ Å, $c = 20.864(2)$ Å, space group $R-3m$ (166), and $Z=3$.

Keywords: Palmierite, x-ray powder diffraction, Rietveld refinement, preferred orientation, synthesis

DISCLAIMER

This report was prepared as an account of work sponsored by an agency of the United States Government. Neither the United States Government nor any agency thereof, nor any of their employees, make any warranty, express or implied, or assumes any legal liability or responsibility for the accuracy, completeness, or usefulness of any information, apparatus, product, or process disclosed, or represents that its use would not infringe privately owned rights. Reference herein to any specific commercial product, process, or service by trade name, trademark, manufacturer, or otherwise does not necessarily constitute or imply its endorsement, recommendation, or favoring by the United States Government or any agency thereof. The views and opinions of authors expressed herein do not necessarily state or reflect those of the United States Government or any agency thereof.

DISCLAIMER

**Portions of this document may be illegible
in electronic image products. Images are
produced from the best available original
document.**

X-ray powder diffraction study of synthetic Palmierite, $K_2Pb(SO_4)_2$

Ralph G. Tissot and Mark A. Rodriguez

Sandia National Laboratories, Materials Characterization Department 1822, Albuquerque, New Mexico, 87185

Diana L. Sipola and James A. Voigt

Sandia National Laboratories, Ceramic Materials Department 1843, Albuquerque, New Mexico, 87185

I. INTRODUCTION

In order to develop a quantitative standard containing $K_2Pb(SO_4)_2$, synthesis of this phase was required. Schwartz, Von H. (1966) described both a thermal and aqueous method of producing a synthetic Palmierite and Saalfeld Von H. (1973) investigated a natural occurring Palmierite from Mount Vesuvius, Italy. An aqueous method for Palmierite synthesis has been developed and is reported here. X-ray powder diffraction of this synthetic Palmierite revealed intensity differences compared to the current ICDD Powder Diffraction File (PDF) No. 29-1015. Modeling of the structure from single crystal data and both Rietveld and least-square refinements also showed differences in intensity compared to PDF 29-1015. This study examines these differences and shows that the powder diffraction intensities presented here more closely match with predicted by modeling and structure refinements. Additionally, we discuss possible reasons for intensity deviation, including preferred orientation and chemical inhomogeneity.

II. EXPERIMENTAL PROCEDURES

Sample Synthesis: The synthesis was conducted with a large excess of K to Pb (4.19 moles K per mole of Pb) to promote the formation of $K_2Pb(SO_4)_2$ rather than $PbSO_4$. Fisher Scientific certified A.C.S. $Pb(NO_3)_2$ and K_2SO_4 salts were used. The salts were dissolved in deionized water. The individual salt solutions were filtered through 0.45 μm filter paper prior to the reaction, the lead nitrate solution being filtered twice. The reaction was batched to synthesize 20g $K_2Pb(SO_4)_2$. The $Pb(NO_3)_2$ solution contained 0.04192 moles Pb (108.3g prefiltered solution). The K_2SO_4 solution contained 0.1758 moles K (205.7g prefiltered solution). The pH of the K_2SO_4 solution was ~6.1.

The equipment used for the reaction included a 500 mL three neck round bottom flask, a condensor, a heating mantle, and a 50 mL buret used for solution addition. The $Pb(NO_3)_2$ solution was slowly dripped from the buret over 37 minutes into the K_2SO_4 solution held at 80.5°C to 84°C. Upon completion of the lead nitrate addition, the

precipitate was stirred for two hours with a temperature ranging from 84°C to 86°C. After the two hour hold, the pH of the slurry product was ~5.2 when taken at ~84°C.

The precipitate was isolated by vacuum filtration at the elevated temperature using a Buchner funnel with type P-2 filter paper. The precipitate was transferred to a second filter apparatus equipped with a 0.45 μm filter paper. It was washed with 82g deionized water, 50 mL of a solution of 50:50 water:methanol, and 30 mL methanol (100%). The vacuum filtration was very slow, so the precipitate was transferred to a 60 mL glass frit funnel for a final wash with 70 mL methanol. The powder was dried at ~89°C overnight. The amount of powder collected was 18.5g, resulting in ~92.5% yield. This powder shall be referred to hereafter as the "as-prepared" Palmierite powder.

In order to remove most the preferred orientation effects observed in initial XRD scans of the as-prepared Palmierite powder, a portion of this powder was placed in a crucible (uncovered) and melted in a Thermolyne 6000 furnace at 760°C for 20 minutes. The resulting powder did not completely melt; instead, large agglomerates formed during sintering. This material was ground to a fine powder in an agate mortar and pestle and then heat treated in a crucible (uncovered) at 450°C for 8 hours. This resulting powder shall hereafter be referred to as the "annealed" Palmierite powder.

Specimen Preparation: A portion of both Palmierite samples were ground in an agate mortar and pestle and sifted from a 60 mesh screen onto a lightly greased "zero background" slide as outlined by Jenkins & Snyder (1996). The slide was lightly tapped to remove the excess specimen.

The morphology and crystallite size were observed and determined using a scanning electron microscope (SEM, Joel 6400XV and Hitachi S4500FE). The specimen powders were prepared for SEM analysis by coating each with a thin gold/palladium layer to prevent specimen charging under the electron beam. The composition of the specimen was confirmed by electron microprobe analysis (EMPA, Joel 8600). The specimens were prepared for EMPA by mixing the powders in epoxy, polishing and then carbon coated to prevent electron beam charging.

Data Collection: A Siemens D500 θ/θ powder diffractometer was used for data collection. The data was collected over a scan range of 10-125° 2θ at a step size of 0.05° 2θ and a dwell time of 22sec. Monochromatic Cu $\text{K}\alpha$ (0.15406nm) radiation was produced using a diffracted beam curved graphite monochrometer. Fixed slits of 1.0, 1.0, 1.0, 0.15, & 0.15 degrees were used. The instrument power was 45kV and 30mA. Alignment and calibration were checked using a LaB₆ (NIST SRM660) external standard. Diffraction data were collected at room temperature (25°C). Datascan V3.1 (Materials Data Inc.) software was used to operating the diffractometer.

RECEIVED

JAN 09 2001

ESTI

III. RESULTS AND DISCUSSION

Initially, the as-prepared Palmierite was used for generating the powder diffraction data. Subsequent analysis of the resulting Palmierite powder pattern showed intensities consistent with a high degree of (00l) preferred orientation as seen by an unusually large (003) reflection. Hence, it was thought that heat treatment of the sample might change the powder morphology, and thereby, reduce the preferred orientation effects. Evaluation of the diffraction data for the annealed powder showed a significant reduction in the (003) intensity, however the (003) relative intensity was still high compared to the published card (29-1015). At this point suspicions concerning the reported intensities in the published card warranted a more detailed investigation.

We were successful in collecting single crystal data on one of the as-prepared Palmierite crystals. Complete absorption correction on the single crystal proved quite difficult due to its very high aspect ratio. However, refinement of the atom positions for $K_2Pb(SO_4)_2$ worked quite well. These fractional coordinates and thermal parameters were used along with the refined unit cell parameters from the powder data to generate a calculated pattern using the program RUBY (Materials Data, Inc.). Parameters used for the calculated pattern were as follows: $\lambda = 0.1540589$ nm, a Modified Lorentzian peak shape with $K_{\alpha 1} + K_{\alpha 2}$ doublets, and neutral scattering factors for Pb, K, S, and O atoms taken directly from the International Tables for X-ray Crystallography (1974). Diffraction data for the calculated structure are shown in Table 1. Interestingly, the predicted relative intensity for the (003) in the calculated pattern is 52%, while the PDF card 29-1015 value lists as 35%. This is a significant discrepancy. Using the calculated pattern as a guide, we re-evaluated our powder data to determine which data sets most closely matched the predicted intensities. Figure 1 shows the first six Palmierite reflections for four diffraction patterns: a pattern generated from PDF card 29-1015, a calculated pattern based on our single crystal work, and observed patterns for the as-prepared and annealed powders. As one can see, there are inconsistencies in the peak intensities between the PDF card 29-1015 and that of the calculated pattern. Significant variation is also observed in the as-prepared powder (003) reflection as compared to the calculated pattern. To quantify our evaluation, we performed two different peak intensity determination methods on the as-prepared and annealed powders and then compared them to the calculated intensities. The first method was the standard peak-finder routine in the JADE software (Materials Data, Inc.). Second, we performed a Rietveld refinement on the data sets including a modeling of the preferred orientation vector along the (003). Results of the relative peak intensities for the first six reflections are shown in Table 2. The last row in the table, called $\Sigma|\%Error|$, is the total of the absolute error between the calculated and observed intensities for the six listed reflections. The smaller the

$\Sigma|\%Error|$, the better the data matched the calculated pattern. The results show that for both the peak-finder and Rietveld methods, the as-prepared Palmierite has a much larger $\Sigma|\%Error|$ than the annealed Palmierite. As expected, the peak finder routine showed a much larger peak intensity deviation than that observed for the Rietveld refinement. The large deviations seen in the as-prepared Palmierite can be attributed to preferred orientation. Figure 2 shows the SEM micrograph of the as-prepared Palmierite powder. The crystallites have a distinct hexagonal plate-like morphology and a very large aspect ratio suggesting the high basal plane (00ℓ) orientation found in the initial powder pattern. The observed mean crystallite size is 3-6 μm . Figure 3 is a micrograph of the annealed Palmierite powder showing a less defined morphology with several large crystal agglomerates but a smaller overall crystallite size. The heat treatment of the powder has significantly reduced the aspect ratio of the crystals, thereby improving the random nature of the diffraction pattern as indicated in Figure 1 and Table 2. Although careful specimen preparation methods were used, it was still difficult to remove all the preferred orientation effects. This was evident in the Rietveld refinement results for the two samples that still showed slight preferred orientation present along the (003) orientation vector using the March model as outlined by March (1932) and Dollase (1986). The as-prepared Palmierite orientation vector refined to a value of 0.953 while the annealed Palmierite was much closer to random at 0.984. Based on these observations, it was concluded that the new card data should be calculated based on the annealed Palmierite powder. More detail concerning the Rietveld refinement methodology is given later.

To generate a new powder diffraction card for Palmerite, all the reflections except those of the trace impurity phase $\text{Pb}(\text{SO}_4)_2$ were fitted using the least-squares refinement program with in the JADE (Materials Data, Inc.) software package. The Smith and Snyder (1979) figure of merit for the refinement is $F_{30} = 83.4(36)$ with a $|2\theta| = 0.0107^\circ$. Although it is not the main focus of this paper to improve the peak 2θ positions, we were successful in reducing the $|2\theta|$ by 0.0036° from the original value of $|2\theta| = 0.0143^\circ$ reported in PDF card 29-1015. X-ray powder diffraction data for Palmierite are given in Table 3.

To investigate possible origins of the intensity variations in PDF card 29-1015 we considered the effects of preferred orientation and chemical inhomogeneity. For the case of preferred orientation, we did observe dramatic increases in the (003) reflection for the as-prepared powder. However, in all our XRD analysis we never observed the (003) reflection dropping significantly below the calculated relative intensity of ~52%. Hence, we reasoned that preferred orientation did not correlate well with the reduced intensities for the (003), (101), and (012) peaks as reported in PDF card 29-1015. Next, we investigated the possibility of chemical inhomogeneity. We generated calculated patterns

on structures with varying Pb and K occupancy and were successful in generating the observed peak intensities reported in PDF card 29-1015 by reducing the Pb occupancy by ~10-20%. Rietveld refinement on a pattern generated from the PDF card 29-1015 also indicated a significant reduction in Pb site occupancy confirming our observations from the calculated patterns. Hence, it appears that the original specimen may contain Pb vacancies resulting from Pb volatility during sample preparation or perhaps cation disorder between the K and Pb layers. Another possibility could be that an additional cation is present in the Pb site (e.g., Ca, or Na) that has the net effect of substantially reducing the scattering factor from the Pb site. It is difficult to access the real reason, but it appears likely that some chemical variation from the $K_2Pb(SO_4)_2$ composition is the source of the peak intensity discrepancy.

Therefore, it was considered paramount to diagnose the chemical composition of the samples to confirm the proper stoichiometry. Electron Microprobe analysis (EMPA) for both the as-prepared and annealed Palmierite samples in our investigation confirmed the K:Pb:S ratio as 2:1:2 within experimental error. This is consistent with the Palmierite composition $K_2Pb(SO_4)_2$.

Having confirmed the proper chemical composition for this phase via EMPA, Rietveld structure refinement was performed to confirm the Pb and K site occupancy as well as check for any possible site mixing of the Pb and K atoms. Crystal structure refinement was carried out using Rietveld's method with the program RIQAS (Materials Data, Inc.). Initial unit cell parameters were obtained from our earlier single crystal work. Conditions for the refinement are listed in Table 4. A total of 20 parameters including 7 structural parameters were refined. The atomic scattering factors for Pb, K, S, and O were taken from the International Table for X-ray Crystallography IV (1974). Crystal data for both the least-squares refinement and the Rietveld refinement are shown in Table 5 for comparison purposes. Unit cell parameters obtained using the least-squares refinement method are in good agreement with those obtained in the Rietveld refinement. Atom fractional coordinates and site occupancies for the Rietveld refinement of annealed Palmierite are given in Tables 6. According to this table, Pb and K sites refined to full occupancy indicating that the structure is well ordered with no apparent cation deficiency or site mixing occurring. This is consistent with the EMPA analysis of the powder. Temperature parameters for all atoms were fixed at a $B_{iso} = 1.0$. An overall temperature parameter, B , was refined as reported in Table 5. This value tended to be a little high due to the roughness of the specimen on the zero-background sample holder. Figure 4 shows the results of the fit for the Rietveld refinement of the annealed powder. The calculated and observed patterns are well matched and the difference pattern appears to be relatively free of large intensity variations. Low residual error values ($R_p = 7.24\%$

as reported in Table 4) indicated a good fit for the refinement. A packing diagram for the structure is shown in Figure 6. This plot illustrates the layered type behavior of the unit cell, with distorted Pb-O octahedra and SO₄ tetrahedra making up a slab-type layer. K incorporates in-between these slab layers in two offsetting K layers, interacting with O atoms from each slab. The Pb atoms are shown incorporated into distorted PbO₆ octahedra for the purpose of showing the connectivity of the Pb-O and S-O bonds in the slab layer. In reality the Pb has additional interaction with six more oxygen atoms at longer distances (~3.1 Å) giving it an overall coordination of 12.

IV. ACKNOWLEDGEMENTS

The United States Department of Energy supported this work under Contract DE-AC04-94AL85000. Sandia is a multi-program laboratory operated by Sandia Corporation, a Lockheed Martin Company, for the United States Department of Energy.

The authors would like to acknowledge Alice Kilgo and Paul Hlava; Sandia's Materials Characterization Department 1822, for the EMPA sample preparation and analysis respectively. Also a special thanks to Francois Bonhomme; Sandia's Environmental Monitoring and Characterization Department 6233, for the Palmierite packing diagram.

V. REFERENCES

Dollase, W. A. (1986), *J. Appl. Crystallogr.* **19**, 267-272.

International Tables for X-ray Crystallography (1974). Vol. IV. (Kluwer Academic, Boston), pp. 71.

Jenkins, R, and Snyder, R. L. (1996), *Introduction to X-Ray Powder Diffractometry* (Wiley, New York), pp.149-150.

March, A. (1932). *Z. Kristallogr.*, **81**, 285-297.

Saalfeld, H. (1973). "Crystallographic Investigations of Glaserite from Mount Vesuvius (Italy)," *Neues Jahrb. Mineral.* **2**, 75-78

Schwarz, H. (1966). "I. Sulfate," *Z. Anorg. Allg. Chem.* **344**, 41-55

Smith, G. S., and Snyder, R. L. (1979). "F(N): A Criterion for Rating Powder Diffraction Patterns and Evaluating the Reliability of Powder Pattern Indexing," *J. Appl. Crystallogr.* **12**, 60-65.

TABLE 1. Calculated powder pattern for Palmierite

hkl	$2\theta_{\text{calc}}$	d_{calc}	I/I_0
0 0 3	12.720	6.9537	52
1 0 1	19.108	4.6410	38
0 1 2	20.492	4.3306	61
1 0 4	25.311	3.5159	19
0 0 6	25.600	3.4768	4
0 1 5	28.423	3.1376	100
1 1 0	32.553	2.7483	76
1 1 3	35.080	2.5560	36
1 0 7	35.511	2.5260	14
0 2 1	38.020	2.3648	10
2 0 2	38.775	2.3205	1
0 0 9	38.820	2.3179	9
0 1 8	39.366	2.2870	3
0 2 4	41.678	2.1653	19
1 1 6	41.865	2.1561	29
2 0 5	43.752	2.0674	32
1 0 10	47.551	1.9107	23
0 2 7	48.936	1.8598	2
2 1 1	50.900	1.7926	11
1 2 2	51.501	1.7730	9
1 1 9	51.537	1.7719	13
0 1 11	51.854	1.7618	4
2 0 8	51.976	1.7579	7
0 0 12	52.604	1.7384	3
2 1 4	53.859	1.7008	5
1 2 5	55.581	1.6521	20
3 0 0	58.084	1.5868	11
0 2 10	58.814	1.5688	7
3 0 3	59.727	1.5470	5
0 3 3	59.727	1.5470	2
2 1 7	60.014	1.5403	4
1 0 13	60.871	1.5206	1
2 0 11	62.577	1.4832	1
1 2 8	62.685	1.4809	3
1 1 12	63.243	1.4692	5
0 3 6	64.501	1.4435	4
3 0 6	64.501	1.4435	3
0 1 14	65.597	1.4220	3
0 0 15	67.267	1.3907	2
2 2 0	68.188	1.3742	11
2 1 10	68.856	1.3625	14
2 2 3	69.695	1.3481	3
0 2 13	70.752	1.3305	2
1 3 1	71.551	1.3176	2
3 1 2	72.044	1.3098	3
3 0 9	72.074	1.3093	2
0 3 9	72.074	1.3093	3
1 2 11	72.335	1.3053	3
1 3 4	74.005	1.2799	2
2 2 6	74.134	1.2780	2
2 0 14	75.165	1.2630	1
3 1 5	75.462	1.2587	9
1 0 16	75.550	1.2575	1
1 1 15	76.743	1.2409	11
1 3 7	79.306	1.2071	2

TABLE 2. Comparison of peak intensity results from calculated, as prepared, and annealed powders.

(hkl)	I(%) Calc. pattern	I(%) PDF card 29-1015	I (%) As Prepared Peak finder	I(%) As Prepared Rietveld	I(%) Annealed Peak finder	I(%) Annealed Rietveld
(003)	52	35	84	75	46	52
(101)	38	25	45	40	35	35
(012)	61	45	67	63	59	56
(104)	19	18	17	19	18	18
(006)	4	3	4	5	4	3
(105)	100	100	100	100	100	100
$\Sigma \% \text{Error} $	-	48	47	18	12	10

TABLE 3. X-ray powder diffraction data for heated Palmierite. Radiation: Cu K α_1 (0.15406nm)

<i>hkl</i>	2 θ (obs.)	2 θ (cal.)	<i>d</i> (obs.)	<i>I/I₀</i> (%)
0 0 3	12.789	12.718	6.916	46.1
1 0 1	19.185	19.105	4.622	34.8
0 1 2	20.560	20.488	4.316	58.8
1 0 4	25.394	25.307	3.505	18.0
0 0 6	25.654	25.596	3.470	3.8
0 1 5	28.505	28.418	3.139	100.0
1 1 0	32.643	32.548	2.741	71.3
1 1 3	35.163	35.074	2.550	30.9
1 0 7	35.600	35.504	2.520	11.9
0 2 1	38.105	38.014	2.360	7.5
0 0 9	38.905	38.813	2.313	8.4
0 1 8	39.458	39.359	2.282	2.3
0 2 4		41.671		
1 1 6	41.940	41.857	2.152	23.9
2 0 5	43.821	43.744	2.064	23.7
1 1 10	47.647	47.542	1.907	18.3
0 2 7	49.012	48.927	1.857	1.4
2 1 1	50.971	50.891	1.790	6.6
1 2 2	51.610	51.492	1.770	12.7
0 1 11		51.844		
2 0 8	52.046	51.966	1.756	4.7
0 0 12	52.667	52.594	1.737	2.9
2 1 4	53.918	53.849	1.699	2.8
1 2 5	55.659	55.571	1.650	13.8
3 0 0	58.162	58.074	1.585	6.6
0 2 10	58.874	58.802	1.567	3.6
3 0 3	59.804	59.716	1.545	3.7
2 1 7		60.003		
1 0 13	60.957	60.859	1.518	0.7
2 0 11		62.565		
1 2 8	62.742	62.673	1.480	1.6
1 1 12	63.312	63.230	1.468	3.1
3 0 6	64.559	64.489	1.442	3.8
0 1 14	65.656	65.584	1.421	1.4
0 0 15	67.246	67.253	1.389	1.3
2 2 0	68.252	68.176	1.373	4.4
2 1 10	68.913	68.842	1.361	7.5
2 2 3	69.754	69.682	1.347	1.5
0 2 13	70.804	70.737	1.330	1.0
1 3 1	71.640	71.537	1.316	0.8
3 0 9	72.116	72.060	1.309	3.1
1 2 11	72.382	72.321	1.305	1.2
1 3 4		73.991		
2 0 14		75.149		
3 1 5	75.537	75.448	1.258	4.4
1 1 15	76.800	76.726	1.240	5.9
1 3 7	79.359	79.290	1.206	0.9
2 1 13	80.131	80.047	1.196	0.5
4 0 1	80.847	80.815	1.188	0.5
0 4 2	81.367	81.289	1.182	1.7

TABLE 4. Experimental Conditions for Rietveld refinement of annealed Palmierite

formula weight	483.57
2θ range for Rietveld refinement (degrees)	15 - 120
number of reflections in the 2θ range	128
preferred orientation vector along (003)	0.984(3)
overall Temperature parameter B , (\AA^2)	1.99(4)
Peak shape function	Pearson VII, (4 parameters)
Background function	Complex polynomial, n=5
Temperature (°C)	25
R_p	0.0724
R_{wp}	0.1256
R_e	0.0771

TABLE 5. Crystal structure data for Palmierite.

Crystal System	Trigonal/Hexagonal	
Space Group	R-3 m (#166)	
Formula number in unit cell	Z = 3	
	Least Squares method	Rietveld method
a axis (\AA)	5.497(1)	5.497(1)
c axis (\AA)	20.864(2)	20.861(3)
Unit cell volume (\AA^3)	546.1(5)	545.8(5)
D_x (g/cm 3)	4.36(5)	4.41(3)

TABLE 6. Positional Parameters for annealed Palmierite

Atom	x	y	z	Occ.
K	1/3	2/3	0.4650(4)	1.01(2)
Pb	0	0	0	1.03(3)
S	0	0	0.4033(4)	1
O(1)	0	0	0.333(2)	1
O(2)	0.296	0.148	0.427	1

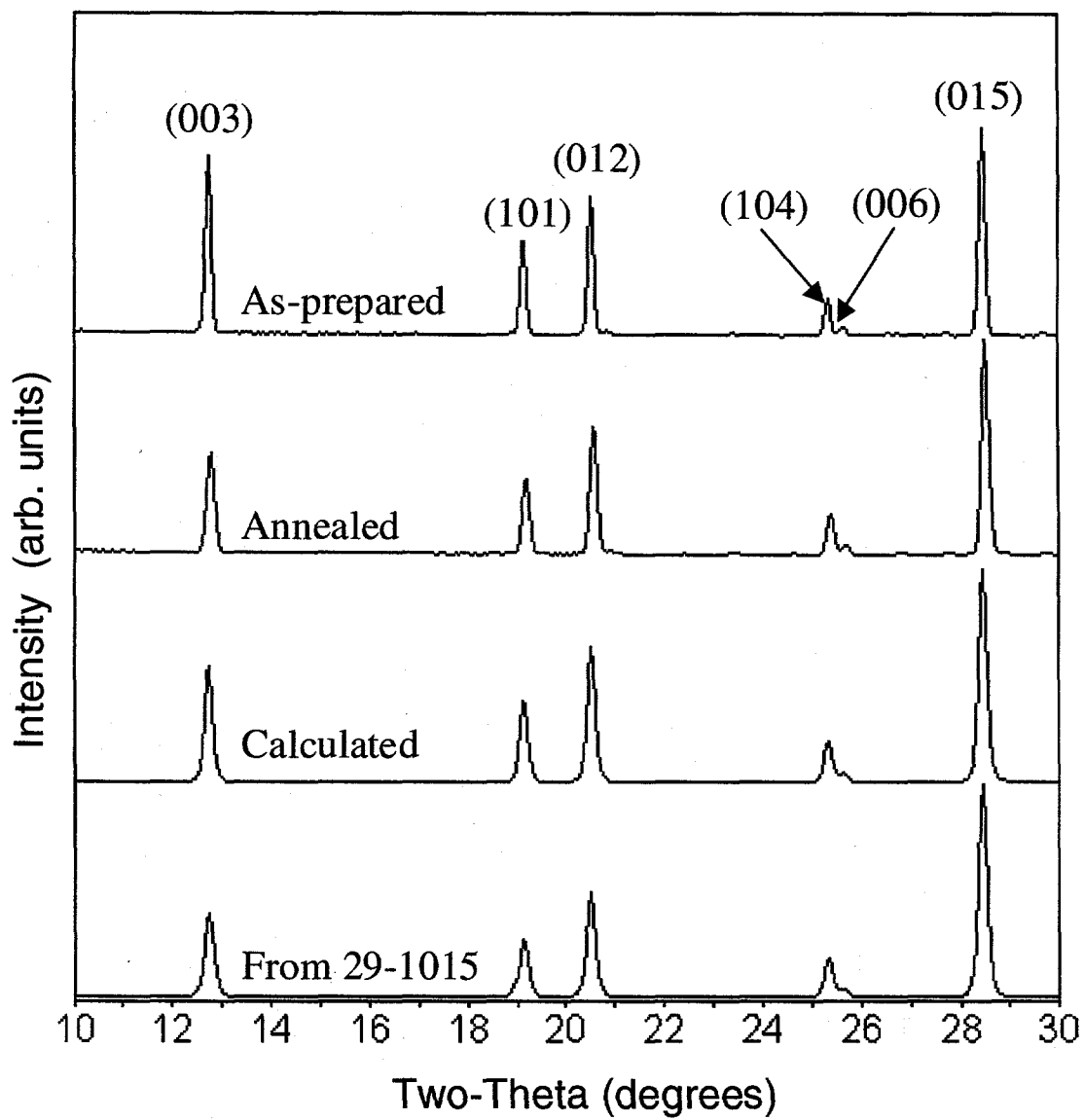


FIGURE 1. Comparison of the calculated $\text{K}_2\text{Pb}(\text{SO}_4)_2$ pattern to observed diffraction data for the as-prepared and annealed powders. An additional pattern generated from the PDF card 29-1015 is also given.

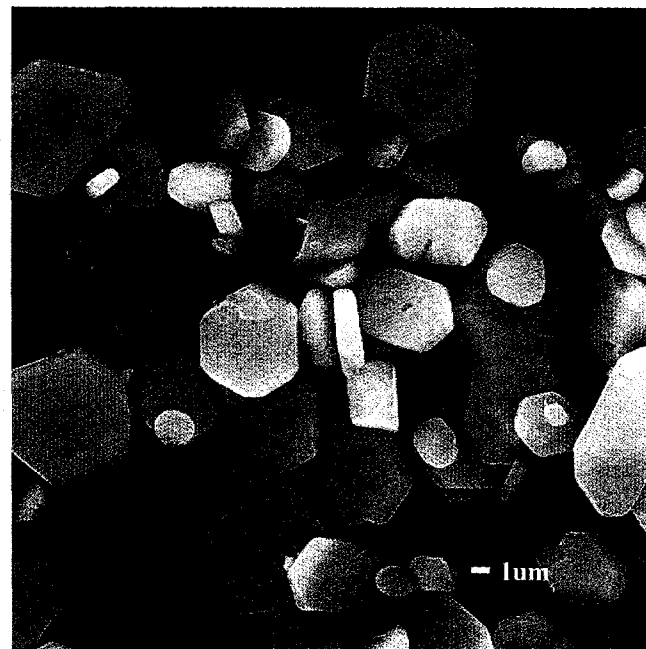


FIGURE 2. SEM micrograph of as-prepared Palmierite particles.

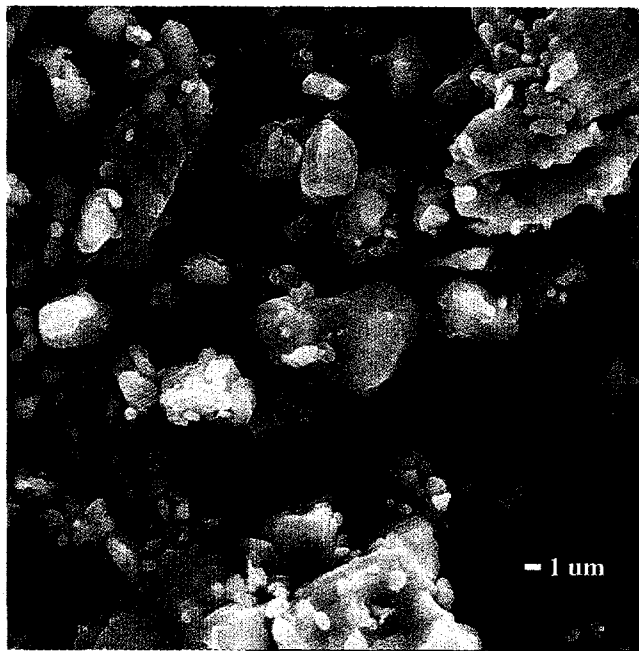


FIGURE 3. SEM micrograph of annealed Palmierite particles.

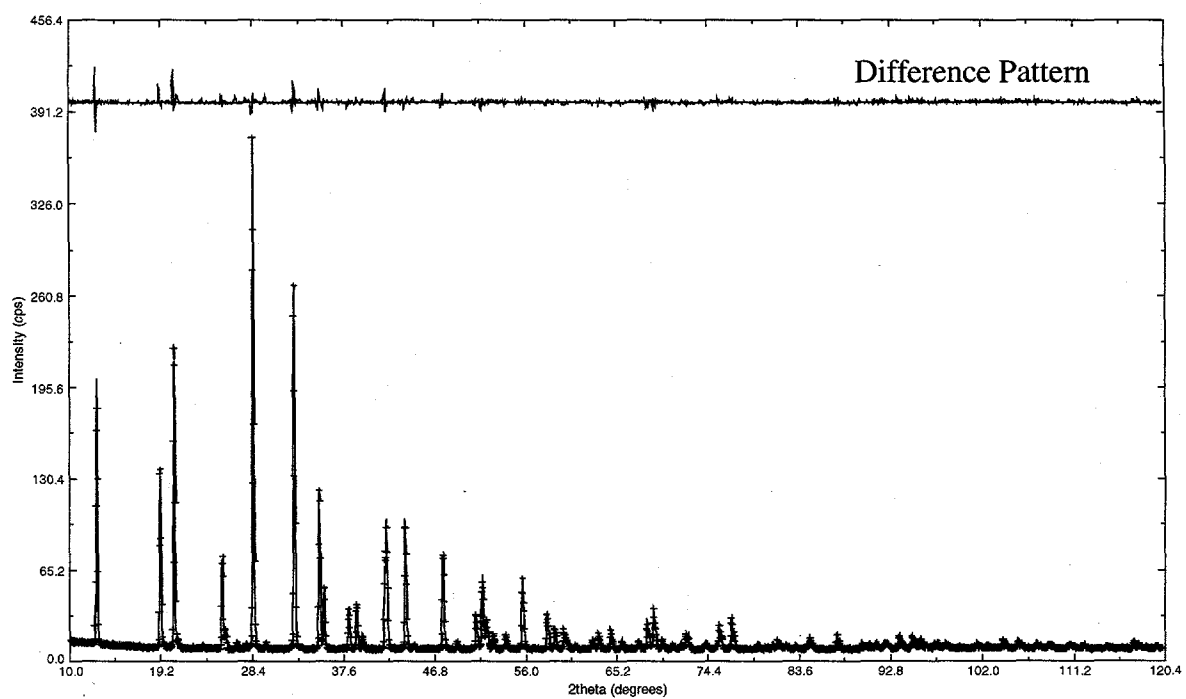


FIGURE 4. Rietveld refinement $\text{K}_2\text{Pb}(\text{SO}_4)_2$ from annealed powder.

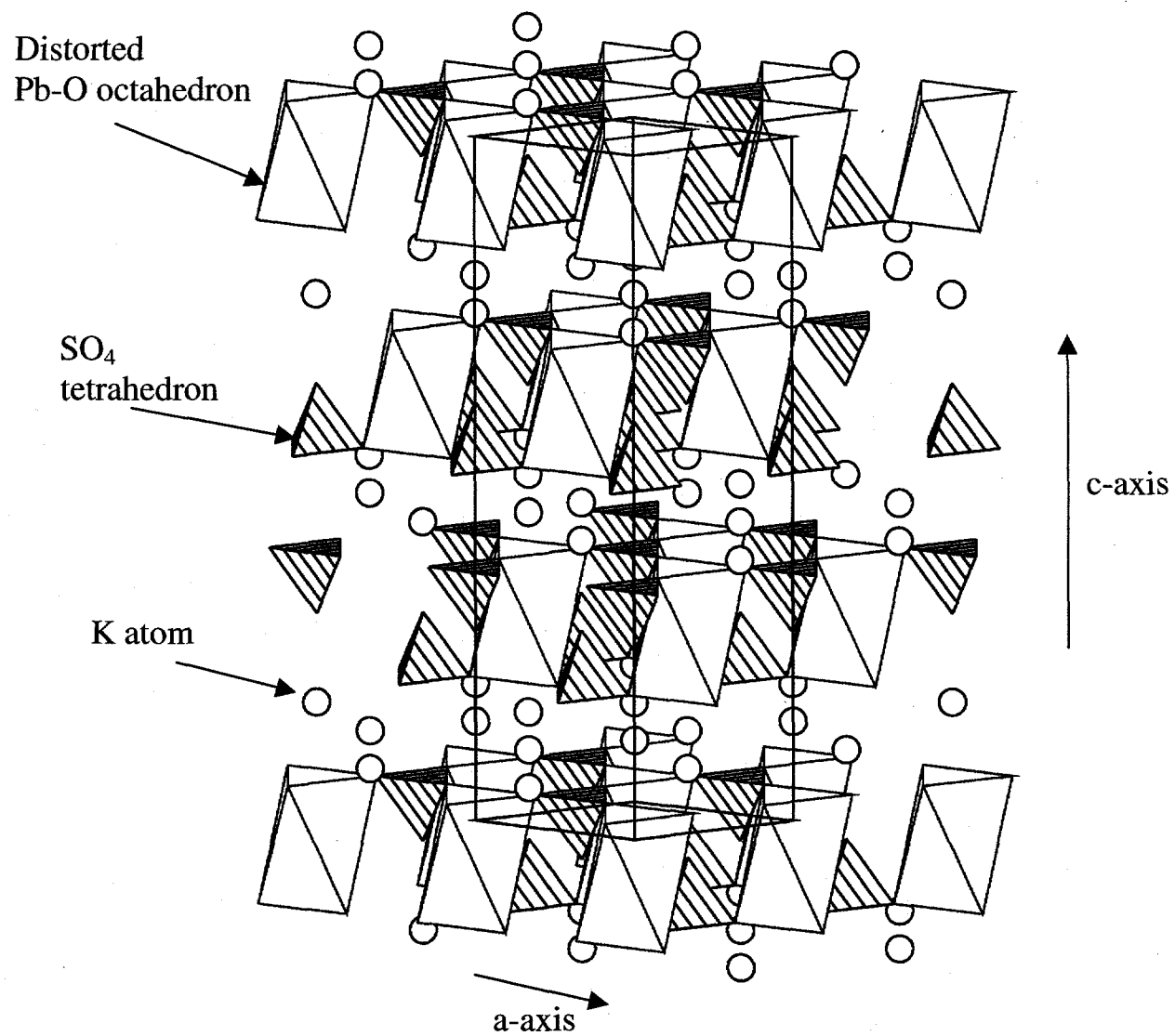


FIGURE 5. Packing diagram of $\text{K}_2\text{Pb}(\text{SO}_4)_2$ structure showing SO_4 tetrahedra and distorted PbO_6 octahedra.